Achievements in the Life Sciences 8 (2014) 101–111

HOSTED BY

ELSEVIER

Contents lists available at ScienceDirect

Achievements in the Life Sciences

journal homepage: www.elsevier.com/locate/als

# Effects of Lithium Nano-Scaled Particles on Local and Systemic Structural and Functional Organism Transformations Under Tumour Growth

Natalya P. Bgatova *, Olga P. Makarova, Anastasiya A. Pozhidayeva, Yurii I. Borodin, Lubov N. Rachkovskaya, Vladimir I. Konenkov

*Scientific Institution of Clinical and Experimental Lymphology, Siberian Branch the Russian Academy of Medical Sciences, Novosibirsk, Russian Federation*

ARTICLE INFO

Available online 12 March 2015

*Keywords:*
Lithium carbonate nano-scaled particles
Hepatocellular carcinoma
Lipid peroxidation
Necrosis
Organ structure

ABSTRACT

The results of a study of structural and metabolic changes in CBA mice with hepatocellular carcinoma caused by lithium carbonate nano-sized particles are presented. Light microscopy, electron microscopy and other biochemical methods were used to show that injection of lithium carbonate nano-sized particles to the periphery of the tumour results in enhanced destructive processes within the tumour. The number of neutrophils and macrophages in the tumour increased, whereas the density of blood vessels and haemoglobin concentration were reduced; the extent of tumour necrosis lipid peroxidation and production of nitric oxide was also increased. At the same time, the activity of antioxidant enzymes including superoxide dismutase and catalase remained the same. The introduction of lithium carbonate nano-scaled particles protects vital organs including the heart and lungs from the damaging effect of secondary products of lipid peroxidation.



## Introduction

Hepatocellular carcinoma is one of the most aggressive human tumours. It is the fifth most common cancer and third highest in terms of mortality in the world (Pang and Poon, 2012; Shen and Cao, 2012). Standard medical treatments of hepatocellular cancer include surgical resection, ethanol or radiofrequency ablation (Zhang et al., 2009). Radiofrequency ablation and ethanol ablation are recognized as effective treatment for small encapsulated hepatocellular carcinomas with a diameter less than 3 cm. However, most patients have larger tumours at the moment of detection, and resection of tumours located near great vessels or the bile ducts is not performed.

It is rare for large tumours to respond to treatment with radiofrequency or chemical ablation, and it is almost impossible to secure whole ablation using these methods. During the late stage of disease, embolization (transcatheter arterial chemoembolization, TACE) can be applied, which is performed by the introduction of a chemotherapeutical drug into the hepatic artery (Tono et al., 2013). During this procedure, drugs, which block growth of blood vessels (Sorafenib, Avastin) (Lee et al., 2014), or drugs which affect the cell cycle and stimulate apoptosis of cancer cells (Doxorubicin, Cisplatin, 5-FU) (Kudo, 2012) are used. Although useful, chemotherapeutic drugs have a disadvantage: the development of side effects. Of note are the negative consequences of using cell cycle blocking drugs,

* Corresponding author.

http://dx.doi.org/10.1016/j.als.2015.01.003

particularly Doxorubicin, which causes numerous effects. These effects include cytotoxicity of the drug and its metabolites on liver cells (predominantly on hepatocytes), evident haemodynamic abnormalities in greater circulation (Nepomnyashchikh et al., 2006) and considerable toxic influence on other organ systems, specifically cardiovascular (Nepomnyashchikh et al., 2005).

The mechanistic effects of other drugs on tumour growth, including lithium drug, are also known. For example, lithium carbonate is used to enhance traditional thyroid cancer therapy (Tiuryaeva et al., 2010; Wolff et al., 2010) and as a drug contributing to restoration of marrow and blood constituents after chemotherapy. The following effects were noted: normalization of neutrophil content in the blood after radiotherapy and chemotherapy (Hager et al., 2001), restoration of platelet content in the blood (Hager et al., 2002), increased CD34+ cells in the blood during leukaemia (Canales et al., 1999) and enhanced cytokine production during breast cancer (Merendino et al., 1994). There are data on the use of lithium carbonate as a neuroprotective agent for cancer patients; its purpose is to increase quality of life while saving cognition, improving their emotional state (Yang et al., 2007; Khasraw et al., 2012) and preventing peripheral neuropathy development during aggressive courses of chemotherapy (Mo et al., 2012). Recent research has been conducted showing the efficiency of lithium as an agent for tumour growth suppression (Wang et al., 2008; Zhu et al., 2011). Lithium compounds are regarded as potential agents of target therapy, capable of slowing tumour growth. At the same time, with the development of nanotechnology, new, more innovative features of nanoscale structures are being revealed (Golokhvastov et al., 2013). In previous research we revealed biological effects of lithium carbonate nano-scaled particles during their introduction to intact animals (Bgatova et al., 2012). The purpose of this work was to study the influence of lithium carbonate nano-scaled particles on structural and metabolic changes in CBA mice with hepatocellular carcinoma development.

## Methods

Experiments were performed on CBA line male mice from the Institute of Cytology and Genetics SB RAS. Mice weighted 18–20 g and were three months of age. Work with animals was performed according to the principles of humanity stated in directions of EC (86/609/EEC) and Declaration of Helsinki.

To model the tumour process, we used hepatocellular carcinoma-29 (H-29) cells. This tumour can cause considerable decrease in its carriers' body weight and evident symptoms of cachexia. Hepatocellular carcinoma-29 was generated and verified by employees of the Institute of Cytology and Genetics SB RAS and kindly granted for our research (Kaledin et al., 2009). H-29 cells were transferred to the abdominal cavity of CBA line mice. After 10 days, we made intake of ascitic fluid, slurried in 10-fold volume of saline and injected in 0.1 ml into intact animals' right thigh muscle. To study the influence of inorganic nano-scaled particles on tumour development we injected lithium carbonate nano-scaled particles in doses of 0.037 mg per animal once or five times after induction of tumour growth. We made an intake of material on 3, 7, 13 and 30 days after injection of tumour cells. Animals were taken out of experiment under etheric narcosis by cranio-cervical dislocation. We took five animals for each stage of the research.

We took biological samples for light optic research from thigh muscular tissue, regional inguinal lymph node, kidney, liver, hepatic lymph node, hepatocellular carcinoma-29 cells and from ascitic fluid. These samples were fixed in 10% solution of neutral formalin, dehydrated with a number of alcohols with increasing concentration and placed into paraffin. Sections 5–6 μm thick were coloured with Mayer's haematoxylin and eosin and placed into Canada balsam.

To study biological samples using the electron microscope's translucent mode, we fixed them in 1% solution of $OsO_4$ on phosphate buffer ($pH = 7.4$), dehydrated them using increasing concentrations of ethanol and placed into Apon. From derived blocks, we prepared semi-fine sections 1-μm thick, coloured them with toluidine blue and studied them under a light microscope, choosing the tissue areas to further study using an electron microscope. From selected material, we obtained ultrathin sections 35–45 nm thick using ultratome LKB-NOVA. We contrasted these sections with a saturated water solution of uranyl acetate and lead citrate. We then studied the sections using an electron microscope JEM 1010.

Derived microphotos were morphometrized using Image J software. Digital data were processed using generally accepted statistical methods. We calculated arithmetic mean (M), mean sample error (m) and significance level of distance between mean values (p), based on Student's test for confidence level 95% ($p < 0.05$).

Muscular tissue damage degree was estimated by intensity of lipid peroxidation processes. For determination of lipid peroxidation activity, we homogenized samples of right thigh muscular tissue in cold conditions in 2 ml of 0.85% NaCl water solution, which contained 0.1% EDTA, using a Potter homogenizer. Then, we centrifuged samples for 15 min at 4000 rpm. We determined the activity of lipid peroxidation in homogenates by determining the concentration of reaction products of thiobarbituric acid (TBA) (Volchegorsky et al., 2000). The concentration of TBA-active products was estimated at the wavelength of 532 nm and expressed in micromole/kg, considering molar extinction coefficient equal $1.56 \times 10^5$ $mol^{-1}$ $cm^{-1}$. For efficiency estimation of tissue protection from products that can initiate and intensify lipid peroxidation, we studied the state of antioxidant system's enzymatic link by evaluating the level of catalase and superoxide dismutase (SOD) activity.

The function of catalase is to prevent the accumulation of hydrogen peroxide. Hydrogen peroxide is generated during dismutation of superoxide anion and aerobic oxidation of flavoproteins. SOD catalyses dismutation of superoxide radicals, thereby preventing pathogenic effects of reactive oxygen species. Enzymatic reactions can generate low levels of superoxide anion and hydrogen peroxide $H_2O_2$, which usually are not able to initiate directly lipid peroxidation processes. However, as a result of a numerous consecutive reactions with enzymes and metal ions of variable valence, highly reactive compounds possessing energy can be formed, which can result in C – H-bond breakage and primary lipid radicals' formation.

Catalase activity was estimated by the ability of hydrogen peroxide to make a stable dyed complex with molybdenum salts. Measurements were conducted at a wavelength of 410 nm and expressed in U/100 mg of tissue, considering hydrogen peroxides millimolar extinction coefficient equal $22.2 \times 10^3$ $mmol^{-1}$ $cm^{-1}$. Next, we determined SOD activity in tissue homogenates by the ability of

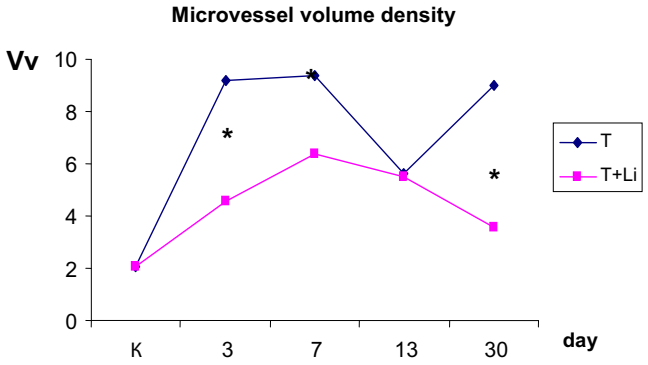


**Fig. 1.** Volume density (Vv) of blood microvessels in tumours. T — tumour; T + Li — 20 days after five-fold injection of lithium carbonate nano-scaled particles on a periphery of tumour growth. * — $P < 0.05$ compared with tumour of control group.

SOD to compete with nitro blue tetrazolium for superoxide radicals; these superoxide radicals were generated as a result of an aerobic interaction between the deoxidised form of nicotinamide adenine dinucleotide (NAD) and phenazine methosulfate. Quantitative characteristics of the progressing reaction were measured at a wavelength of 540 nm. We considered 50% inhibition of nitro blue tetrazolium deoxidation reaction as the activity unit. Enzyme activity was expressed in conventional units (U) per 100 mg of tissue. Protein concentration was measured according to the generally accepted Lowry et al. (1951) method.

Determination of arginase activity was based on carbamide rate of production (Corraliza et al., 1994). We lysed macrophages by freeze-thawing them twice, and then we added 50 μl of 50 mmol Tris–HCl (pH 7.4) and 10 μl of 50 mmol of manganese chloride solution to 50 μl of lysate. Arginase was activated by heating it to 57 °C for 10 min in humid condition, which was obtained by preliminarily wetting of plate lid with Hanks solution. Next, we added 100 μl of 0.5 mol L-arginine solution to each sample and incubated them for 30 min at 37 °C. The reaction was stopped by placing the plate on ice in a refrigerating chamber. Carbamide concentration was estimated by a double enzymatic reaction method. Reaction product quantity was measured via a "SmartSpec Plus" spectrophotometer (Bio-Rad, USA) at a wavelength of 340 nm.

Estimation of haemoglobin in tissue homogenates was conducted according to the haemiglobincyanide method. This method based on the haemoglobin feature, in which it interacts with ferricyanic potassium and haemoglobin oxidizes into methaemoglobin. Methaemoglobin combined with acetone cyanohydrin generates dyed haemiglobincyanide, whose colouring power is proportional to the amount of haemoglobin. Measurement of haemoglobin concentration was performed at a wavelength of 540 nm.

We judged hypoxia development in tumour-bearing muscular tissue by the level of lactate concentration, which was measured by the enzymatic method. This method is based on oxidation of lactic acid into pyruvic by lactate dehydrogenase enzyme simultaneously with deoxidation of nicotinamide adenine nucleotide ($NAD^+$) into NADH. Lactate concentration was determined at a wavelength of 340 nm and was expressed in micromole/g of tissue using a molar extinction coefficient equal to $6.22 \times 10^3\ mol^{-1}\ cm^{-1}$. All measurements were performed using the "SmartSpec Plus" spectrophotometer (Bio-Rad, USA).

Peritoneal macrophages for study were obtained by peritoneal lavage. We injected 7 ml of 199 medium with 10 units/ml of heparin intraperitoneal. After 2 min, we retrieved the macrophages with a syringe cultural medium containing cells of peritoneal exudate. Cell suspensions were washed using the 199 medium with 10 units/ml of heparin centrifuging for 10 min under 1500 rpm. Cell sediment separated via centrifugation was resuspended in DMEM/F12 cultural medium containing 10% of foetal calf serum, 15 mmol

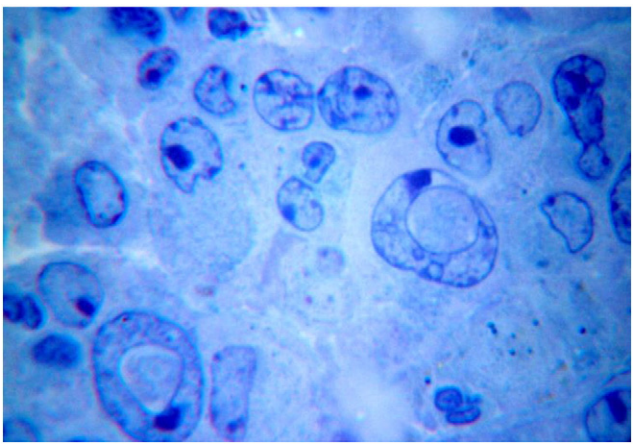

**Fig. 2.** Deformation of tumour cells' nuclei 20 days after five-fold injection of lithium carbonate nano-scaled particles. Toluidine blue stain. Magnification: 10 × 90.

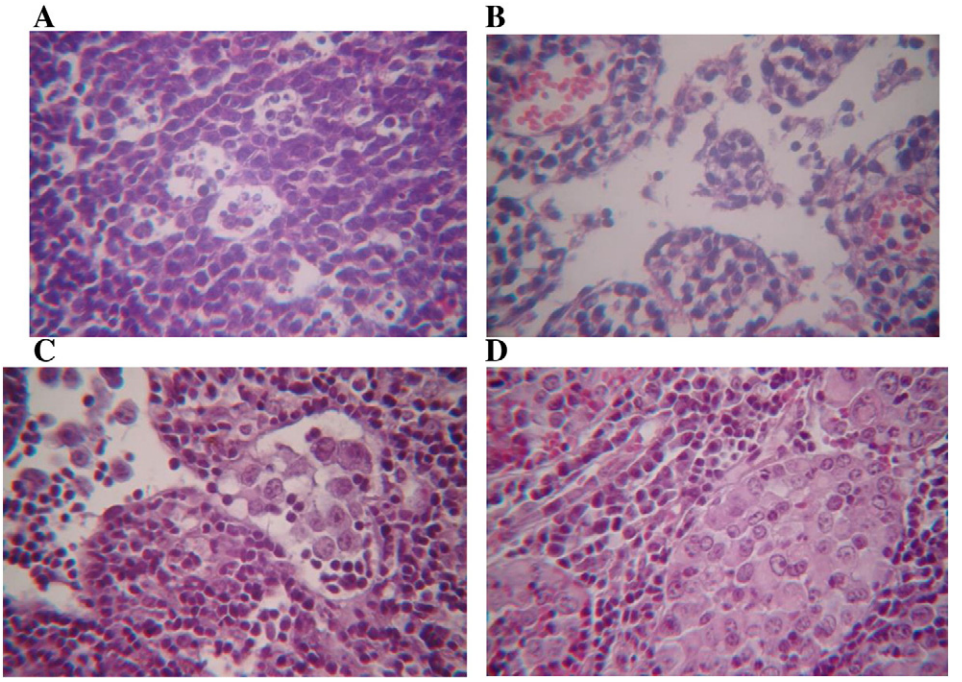


**Fig. 3.** Structure of a mouse regional inguinal lymph node after injection of lithium carbonate nano-scaled particles on the periphery of tumour growth. Haematoxylin and eosin stain. Magnification: 10 × 40. A — Increased content of macrophages in secondary lymphoid follicle after single dose of lithium nano-scaled particles. B — Increased sizes of cerebral sinuses after single dose of lithium carbonate nano-scaled particles. C — Tumour cells in inguinal lymph node sinuses at day 30 of the experiment. D — Replacement of lymphoid parenchyma with tumour cells after 30 days of experiment.

HEPES, 0.3% L-glutamine, and 50 μg/ml gentamicin. To study the peritoneal macrophages, we inserted them into the wells of 96-well plates at a density of $2.0 \times 10^5$ cells in a volume of 200 μl, which was then incubated for 2 h (at 37 °C, 5% $CO_2$). Nonadherent fraction was removed, irrigated twice with a fresh medium and then allowed incubation for 18 additional hours. NO production was estimated by nitrite content (micromole) in the cell culture supernatants. We added 100 μl of Griss reagent to 100 μl of supernatant, mixed it and allowed it to incubate for 15 min before measuring the amount of reaction product using the "SmartSpec Plus" spectrophotometer (Bio-Rad, USA) at a wavelength of 540 nm.

The study of metabolic characteristics was performed in homogenates of the liver and muscular tissues, taken from the area of tumour cell inoculation. Samples of right thigh muscular tissue and liver were homogenized using a Potter homogenizer in cold conditions with 2 ml of 0.85% NaCl water solution, containing 0.1% EDTA. Next, we centrifuged the samples for 15 min at 4000 rpm. Lactic acid concentration was determined using the set of reagents, "Boehringer Mannheim" (Germany). We determined level of triglycerides using the set of reagents, "Vector-Best" (Russia). The level of glycogen was estimated according to the Volchegorsky et al. (2000) method. Activity of arginase and NO was estimated according to the methods described above. To

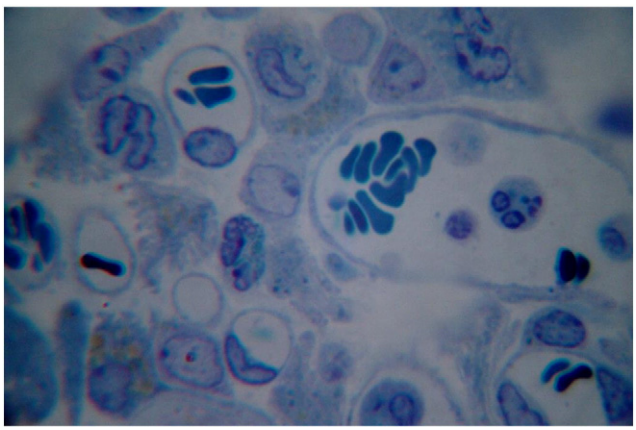

**Fig. 4.** Tumour cells in inguinal lymph node structure 25 days after termination of lithium carbonate particles' injection into the region of tumour growth. Increased content of microvessels, macrophages and neutrophils. Toluidine blue stain. Magnification: 10 × 100.

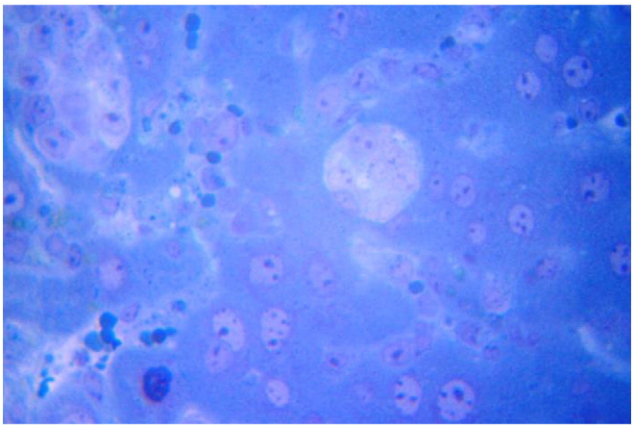

**Fig. 5.** Metastases of tumour cells in the liver and increased content of macrophages, 30 days after transplantation of hepatocellular carcinoma (H-29) cells into the thigh region of experimental animals, against the background of lithium carbonate nano-scaled particle introduction. Toluidine blue stain. Magnification: 10 × 40.

determine NO, we first de-proteinizated tissue homogenate by adding 10% trichloroacetic acid and then centrifuged the sample for 10 min at 3000 rpm. We processed the obtained results using generally accepted methods of variational statistics: dispersion analysis ANOVA and further analysis of batch-to-batch variation using Newman–Keuls test or Mann–Whitney *U*-test.

## Results

After single dosing of lithium carbonate nano-scaled particles, we noted tumour cell necrosis on a periphery of tumour growth and increased content of macrophages in a tumour. Phagosomes with lithium carbonate particles were revealed in the macrophages' cytoplasm. At the same time, no tumour cells necrosis was noted in tumour development without lithium influence, mitosis figures were observed, and quantitative density of macrophages was 40% lower. In this group of animals, 13 days after the start of the experiment, the areas of tumour growth cells were located close and were large in size, and no macrophages were detected in their microenvironment. Determination of blood microvessel volume density in tumours revealed its growth an average of 4.5 times on the third and seventh days of tumour development. Blood microvessel volume density decreased by 40% on the 13th day of the study, exceeding reference level 2.5 times, and increased again by the 30th day of the experiment (Fig. 1).

Within 30 days post-implantation of hepatocellular carcinoma-29 cells into thighs of experimental animals, the tumour cells formed the likeness of hepatic plates, surrounded by “sinusoids”. Tumour cells were large-sized, had a light nuclei with a large nucleolus. By the 30th day of study, animals injected with lithium carbonate nano-scaled particles on a periphery of tumour growth, did not appear to have plate structure of tumour, had lesser observed vasculature development, the presence of macrophages was retained, and tumour cells with deformed vacuolated nuclei were noted (Fig. 2).

In the single dose lithium nano-scaled particle group, we noted a regional inguinal lymph node structure with increased secondary lymphoid follicle number, and increased macrophage numeral density (Fig. 3A). Lymphatic sinuses, especially cerebral, were enlarged (Fig. 3B). During 3–15 days of the experiment, we did not find metastases in a regional inguinal lymph node. Multiple-dose introduction of lithium nano-scaled particles favoured the retention of signs of drainage and detoxification and an increase in organ function, including a considerable dilation of marginal and cerebral sinuses and the growth of macrophages' content in them.

Thirty days after tumour cell implantation, we found metastases in sinuses and lymphoid parenchyma of regional lymph node (Fig. 3C, D). Replacement of lymph node structure by tumour cells indicated the development of the lymph's suppression mechanism.

**Table 1**
The content of TBA-active products in thigh muscular tissue under correction of tumour process by lithium carbonate nano-scaled particles (M ± m).

| Terms of investigation | Animal groups | |
|---|---|---|
| | Tumour | Tumour + $Li_2CO_3$ |
| Intact | 10.86 ± 0.87 (4) | |
| 3 days | 4.47 ± 1.37* (4) | 5.06 ± 1.46* (4) |
| 7 days | 23.2 ± 7.75 (3) | 9.64 ± 1.39+ (5) |
| 13 days | 15.18 ± 1.37*(4) | 10.66 ± 2.12 (4) |
| 33 days | 1.79 (1) | 3.21 (1) |

Comment: the number of animals is included in parentheses.
* $P < 0.05$ compared with control.
\+ $P < 0.05$ compared with the group of animals with spontaneous tumour development.

**Table 2**
The content of catalase and superoxide dismutase in thigh muscular tissue under correction of tumour process by lithium carbonate nano-scaled particles (M ± m).

| Terms of investigation | Catalase (U/100 mg) | | Superoxide dismutase (U/100 mg) | |
|---|---|---|---|---|
| | Tumour | Tumour + $Li_2CO_3$ | Tumour | Tumour + $Li_2CO_3$ |
| Intact | 24.9 ± 7.7 (4) | | 162.9 ± 6.6 (4) | |
| 3 days | 23.7 ± 7.3 (4) | 36.6 ± 12.6 (4) | 152.1 ± 10.4 (4) | 138.4 ± 66.1 (4) |
| 7 days | 12.1 ± 6.5 (3) | 23.7 ± 3.8 (5) | 87.9 ± 19.5* (5) | 74.9 ± 23.4** (3) |
| 13 days | 91.4 ± 12.3* (4) | 95.4 ± 12.8* (4) | 107.2 ± 38.2 (4) | 111.7 ± 35.1 (4) |
| 33 days | 31.0 (1) | 36.4 (1) | 93.1 (1) | 135.4 (1) |

Comment: the number of animals is stated in parentheses.
* $P < 0.05$.
** $P < 0.01$ compared with control.

The unexpected structural changes of the lymph nodes after injection of lithium nano-scaled particles included the considerable increase of macrophages and neutrophil numbers during tumour development and the conditions of lymph node metastasis. Additionally, blood microvessel volume density was increasing significantly in the area of tumour growth (Fig. 4).

Injection of lithium carbonate nano-scaled particles into the tumour growth region set conditions for increasing the macrophage and neutrophil content in the regional structure of the tumour inguinal lymph node, as well as intensified destruction of tumour cells and increased the development of vasculature.

After five-fold dosing of lithium nano-scaled particles into the tumour growth region, we noted stasis of erythrocytes in liver sinusoids. In seven days after five-fold dosing of lithium nano-scaled particles into the tumour, local necrosis was observed in the liver. Stasis of erythrocytes and abundance of monocytes and macrophages were also noted. Twenty-five days after five-fold dosing of lithium nano-scaled particles into the tumour, numerous metastases of different sizes (from one to two cells up to several dozens of polymorphous cells) were noticed in the liver. In addition to metastases, we also recorded multiple macrophages in the parenchyma; many monocytes, macrophages and neutrophils also filled gaps within sinusoids (Fig. 5).

Under the conditions of lithium carbonate nano-scaled particle introduction into the region of tumour growth with developing hepatocellular carcinoma (H-29), the number of macrophages grew in liver sinusoids and parenchyma. Within 30 days of the experiment, regions with metastases in the liver were surrounded by a large number of macrophages. Lithium injection appears to provoke considerable involvement of macrophages to the liver regions of tumour cell migration.

Correction of tumour process, which is developing in right thigh muscle after inoculation of hepatocellular carcinoma (H-29) cells, with injections of lithium carbonate nano-scaled particle suspension directly into affected tissue introduced changes into dynamics of lipid peroxidation processes' activity. Tumour growth in mice under conditions of correction with nano-scaled particles suppressed processes of lipid peroxidation at an early stage and helped prevent spontaneous tumour development (Table 1).

However, during subsequent stages of the investigation, the level of TBA-active products in affected thigh tissue of treated mice returned to the norm. At the same time, animals with spontaneous tumour development had significant accumulation of lipid peroxidation afterproducts. On day 7, animals that were treated with five-fold injection of lithium carbonate nano-scaled particles had 2.4 times less concentration of lipid peroxidation afterproducts compared with indexes, registered for mice with spontaneous tumour development (Table 1). After 13 days, treated animals had the level of TBA-active products within frames of control values, and it was 1.4 times lower than such index for mice with spontaneous hepatocellular carcinoma development. Thereby, the correction of tumour process with lithium carbonate nano-scaled particles considerably inhibited the activity of lipid peroxidation processes in tissue affected with hepatocellular carcinoma (H-29).

**Table 3**
The concentration of TBA-active products in the lungs, heart, liver, kidneys and left thigh muscle of mice with hepatocellular carcinoma H-29 development under correction by lithium carbonate nano-scaled particles (M ± m).

| Organs | Terms of investigation | | | | |
|---|---|---|---|---|---|
| | Intact (4) | Day 3 (4) | Day 7 (3) | Day 13 (4) | Day 33 (1) |
| *Spontaneous development of hepatocellular carcinoma H-29 in the right thigh muscle* | | | | | |
| Thigh without tumour | 10.86 ± 0.87 | | 5.21 ± 0.76* | 3.81 ± 0.62* | 1.79 |
| Lungs | 8.1 ± 0.77 | 10.7 ± 1.73 | 16.42 ± 2.1* | 18.13 ± 3.54 | 22.04 |
| Heart | 10.46 ± 2.68 | 12.1 ± 1.27 | 16.25 ± 1.05* | 11.25 ± 4.13 | 15.38 |
| Liver | 27.21 ± 5.76 | 11.54 ± 3.05* | 16.03 ± 0.53* | 16.37 ± 5.47 | 19.36 |
| Kidneys | 25.98 ± 4.46 | 35.44 ± 7.01 | 18.64 ± 3.31 | 20.49 ± 5.53 | 8.01 |
| *Development of hepatocellular carcinoma H-29 in the right thigh muscle under correction by lithium carbonate nano-scaled particles* | | | | | |
| Thigh without tumour | | | | 3.99 ± 0.89* | 1.51 |
| Lungs | | 22.95 ± 10.04 | 13.41 ± 2.0 | 28.54 ± 12.33 | 13.44 |
| Heart | | 9.2 ± 2.22 | 16.31 ± 2.76 | 12.12 ± 5.42 | 21.23 |
| Liver | | 19.33 ± 6.22 | 20.37 ± 7.04 | 27.1 ± 9.38 | 16.0 |
| Kidneys | | 19.24 ± 3.49 | 17.15 ± 2.33 | 22.58 ± 7.69 | 12.22 |

Comment: the number of animals is stated in parentheses.
* $P < 0.05$ compared with control.

**Table 4**
Catalase activity in the lungs, heart, liver, kidneys and left thigh muscle of mice with hepatocellular carcinoma H-29 development under correction by lithium carbonate nano-scaled particles (M ± m).

| Organs | Terms of investigation | | | | |
|---|---|---|---|---|---|
| | Intact (4) | Day 3 (4) | Day 7 (3) | Day 13 (4) | Day 33 (1) |
| *Spontaneous development of hepatocellular carcinoma H-29 in the right thigh muscle* | | | | | |
| Thigh without tumour | 24.9 ± 7.7 | | | 94.1 ± 11.3* | 30.8 |
| Lungs | 260.8 ± 36.2 | 125.7 ± 9.2* | 124.8 ± 2.0* | 71.21 ± 26.97* | 164.8 |
| Heart | 52.0 ± 4.6 | 4.2 ± 0.8* | 21.7 ± 8.3* | 8.9 ± 3.9* | 76.5 |
| Liver | 110.7 ± 27.9 | 51.6 ± 17.4 | 137.0 ± 13.6 | 43.9 ± 12.4* | 75.2 |
| Kidneys | 168.8 ± 24.5 | 198.5 ± 26.7 | 21.3 ± 10.3* | 246.2 ± 55.3 | 221 |
| *Development of hepatocellular carcinoma H-29 in the right thigh muscle under correction by lithium carbonate nano-scaled particles* | | | | | |
| Thigh without tumour | | | | 94.08 ± 11.9+ | 44.89 |
| Lungs | | 135.2 ± 18.8* | 123.7 ± 4.8** | 94.4 ± 11.9* | 85.1 |
| Heart | | 14.4 ± 3.3*+ | 15.1 ± 4.6** | 15.0 ± 1.7* | 70.8 |
| Liver | | 56.1 ± 19.0 | 183.9 ± 74.6 | 58.6 ± 12.0 | 84.6 |
| Kidneys | | 202.6 ± 11.2 | 39.3 ± 21.1* | 209.6 ± 42.2 | 481.9 |

Comment: the number of animals is stated in parentheses.
* $P < 0.05$.
** $P < 0.01$ compared with control.
\+ $P < 0.05$ in comparison to animals with spontaneous tumour development.

The development of tumour process (13th day), both for treated and non-treated animals, was accompanied by an increase in catalase activity, which is used to eliminate hydrogen peroxide from the tumour cells' microenvironment and to increase tumour cells' active proliferation (Table 2).

The correction of tumour process with lithium nano-sized particles did not influence the level of catalase activity at all stages of investigation. After seven days postinoculation of hepatocellular carcinoma (H-29) cells into the right thigh muscle, we observed a decrease in superoxide dismutase activity, for treated and non-treated animals, which was successfully overcome in both groups of mice by day 13 of tumour process development (Table 3).

It is known, that the content of superoxide dismutase in cells increases in response to increases in superoxide concentration (Menshchikova et al., 2008). Lowered content of superoxide dismutase in tumour cells indicates the inhibition of superoxide's intracellular production. It turned out that double-ply and five-fold introduction of lithium carbonate nano-scaled particles is not able to sufficiently impact the transformation of intracellular metabolic processes associated with the formation and utilization of active oxygen metabolites during tumour development.

During the study of distance effects of lithium carbonate nano-sized particles' multiple-dose introduction under tumour process development, it was found that dynamic changes of activity of lipid peroxidation processes, registered by accumulation of TBA-active products (malondialdehyde) in different parenchymatous organs — the lungs, heart, liver and kidney, were in frames of control values (Table 3).

Thus, correction of tumour process by introduction of lithium carbonate nano-scaled particles promoted the defence of vital organs — the heart and lungs, from damaging effect of lipid peroxidation afterproducts. However, multiple-dose introduction of nano-scaled particles did not influence the decreased level of lipid peroxidation in unaffected muscular tissue of the left thigh, with tumour process development in the right thigh muscle. This is likely to do with the particularities of blood-vascular and functioning of lymphatic vessels.

**Table 5**
Superoxide dismutase activity in the lungs, heart, liver, kidneys and left thigh muscle of mice with hepatocellular carcinoma H-29 development under correction by lithium carbonate nano-scaled particles (M ± m).

| Organs | Terms of investigation | | | | |
|---|---|---|---|---|---|
| | Intact (4) | Day 3 (4) | Day 7 (3) | Day 13 (4) | Day 33 (1) |
| *Spontaneous development of hepatocellular carcinoma H-29 in the right thigh muscle* | | | | | |
| Thigh without tumour | 102.0 ± 37.5 | | | 70.5 ± 9.0 | 151.5 |
| Lungs | 788.8 ± 116.7 | 513.2 ± 58.1 | 547.2 ± 62.9 | 736.1 ± 144.8 | 267.9 |
| Heart | 117.7 ± 30.7 | 133.1 ± 21.6 | 75.6 ± 13.98 | 56.34 ± 5.41 | 12.0 |
| Liver | 92.07 ± 21.34 | 144.1 ± 70.1 | 77.88 ± 40.53 | 171.25 ± 39.5 | 119.5 |
| Kidneys | 142.4 ± 22.02 | 372.4 ± 40.6* | 356.5 ± 22.46* | 483.0 ± 81.4* | 393.8 |
| *Development of hepatocellular carcinoma H-29 in the right thigh muscle under correction by lithium carbonate nano-scaled particles* | | | | | |
| Thigh without tumour | | | | 60.3 ± 28.45 | 140.6 |
| Lungs | | 654.1 ± 218.3 | 439.7 ± 98.37 | 674.1 ± 161.19 | 204.2 |
| Heart | | 125.6 ± 21.92 | 57.21 ± 5.19 | 69.68 ± 7.8 | 228.0 |
| Liver | | 72.12 ± 36.3 | 134.5 ± 61.8 | 187 ± 19.5 | 79.83 |
| Kidneys | | 366.1 ± 16.74* | 367.7 ± 50.72** | 409.2 ± 68.68* | 621.5 |

Comment: the number of animals is stated in parentheses.
* $P < 0.05$.
** $P < 0.01$ compared with control.

**Table 6**
Changes of haemoglobin concentration in the thigh muscle of mice with hepatocellular carcinoma H-29 development under correction by lithium carbonate nano-scaled particles (M ± m).

| Organs | Terms of investigation | | | | |
|---|---|---|---|---|---|
| | Intact | Day 3 (4) | Day 7 | Day 13 | Day 3 |
| Thigh without tumour | | | | 0.57 ± 0.09 (4) | 0.19 (1) |
| Thigh with tumour | | 0.68 ± 0.09* (4) | 0.47 ± 0.04** (5) | 0.67 ± 0.12* (4) | 0.22 (1) |

Comment: the number of animals is stated in parentheses.
* $P < 0.05$.
** $P < 0.01$ compared with control.

Hydroxyl radical and singlet oxygen are highly reactive products that can initiate lipid peroxidation. They have enough energy for release and formation of prime lipid radicals, which originate from rather low-activity superoxide anion-radical, hydrogen peroxide (Menshchikova et al., 2008). Thereby, effects of nano-scaled particles' multiple-dose introduction on lipid peroxidation processes in remote organs, while the tumour process developed in muscular tissue of the right thigh, could be mediated by changing of antioxidant enzymes' activity, which are able to eliminate initial agents in tissues. Thus, the decrease of catalase activity in cardiac muscle under the development of hepatocellular carcinoma (H-29) and with correction using lithium carbonate nano-sized particles, was significantly less expressed on the third day, whereas the rate of catalase activity in the hearts of treated animals exceeded the rate for non-treated animals 3.4 times (Table 4).

We did not register any effects of the treatment on dynamic changes of catalase activity rate in the lungs, liver, kidney and unaffected left thigh muscle under the development of tumour process (Table 4).

There was no noted influence of multiple-dose introduction of lithium nano-scaled particles on the dynamics of superoxide dismutase activity in remote organs — the lungs, heart, liver, kidney and unaffected left thigh muscle (Table 5).

Thereby, introduction of lithium carbonate nano-scaled particles into the thigh muscle caused an increase in lipid peroxidation activity in muscular tissue. This led to alteration within the tissue and the development of inflammatory infiltration, as indicated by an increase in tissue protein concentration. After the development of an inflammatory response to the introduction of lithium carbonate nano-scaled particles, there was a secondary increase in lipid peroxidation activity, leading to a secondary alteration. This secondary alteration included an effect of the release of lysosomal enzymes and active oxygen metabolites from cells, in connective tissue and microvessels. Introduction of lithium carbonate nano-scaled particles provoked the enhancement of catalase activity, which led to dynamic changes of lipid peroxidation intensity, and decrease of superoxide dismutase activity.

Evaluation of haemoglobin concentration revealed that on the third day of hepatocellular carcinoma development, the content of haemoglobin in affected muscle of treated mice was two times higher compared with reference level. At the same time, the content of haemoglobin for untreated mice did not change from the reference level (Table 6).

However, the tumour's systemic action on haemoglobin levels in unaffected muscle of the left thigh at the late stages (13th day) disappeared under treatment. This is possibly indicative of nano-scaled particles indirect effects on decreasing the production of VEGF-A, therefore affecting systemic circulation.

Multiple-dose introduction of lithium carbonate nano-scaled particles most likely contribute to the lower level of vascularisation of hepatocellular carcinoma (H-29) fast-growing tumour node in muscular tissue. This conclusion is based on the lack of significant difference between the content of lactic acid for treated animals from the reference values on the 13th day, whereas non-treated animals had a lactic acid index significantly lower than reference values (Table 7).

Hereby, fast growth of vessels which supply the tumour, leads to a decrease of lactic acid accumulation in affected muscular tissue.

Two-fold introduction of lithium carbonate nano-scaled particles reliably increased the level of nitric oxide production by peritoneal macrophages on day 3 of tumour process development in thigh muscular tissue (Fig. 6).

After introduction of lithium carbonate nano-scaled particles, our results show that the dynamics of lactic acid and triglycerides' content was changing in the area of the muscular tissue inoculated by tumour cells. In cases of hepatocellular carcinoma development without influence of lithium, lipid accumulation in muscular tissue occurs slowly, growing by the 13th day. In contrast, triglyceride levels in treated mice on the third day after tumour process induction increased 4.7 times compared with the reference values, which also exceeded rates in the animal group without impact by 1.7 times (Fig. 7). This finding correlates with previous research showing that after addition of conjugate linoleic acid to hepatocellular carcinoma HepG2 culture, the inhibition of tumour cell

**Table 7**
Change of lactate concentration in the thigh muscle of mice with spontaneous hepatocellular carcinoma H-29 development and under correction by lithium carbonate nano-scaled particles (M ± m).

| Animal groups | Stages of investigation | | | |
|---|---|---|---|---|
| | Intact | Day 3 (4) | Day 13 | Day 3 |
| Spontaneous development | 2.33 ± 0.05 (4) | 3.50 ± 0.63 (4) | 1.33 ± 0.11* (4) | 2.18 (1) |
| Under correction by lithium carbonate nano-scaled particles | | 4.91 ± 2.25 (4) | 1.61 ± 0.37 (4) | 2.79 (1) |

Comment: the number of animals is stated in parentheses.
* $P < 0.05$ compared with control.

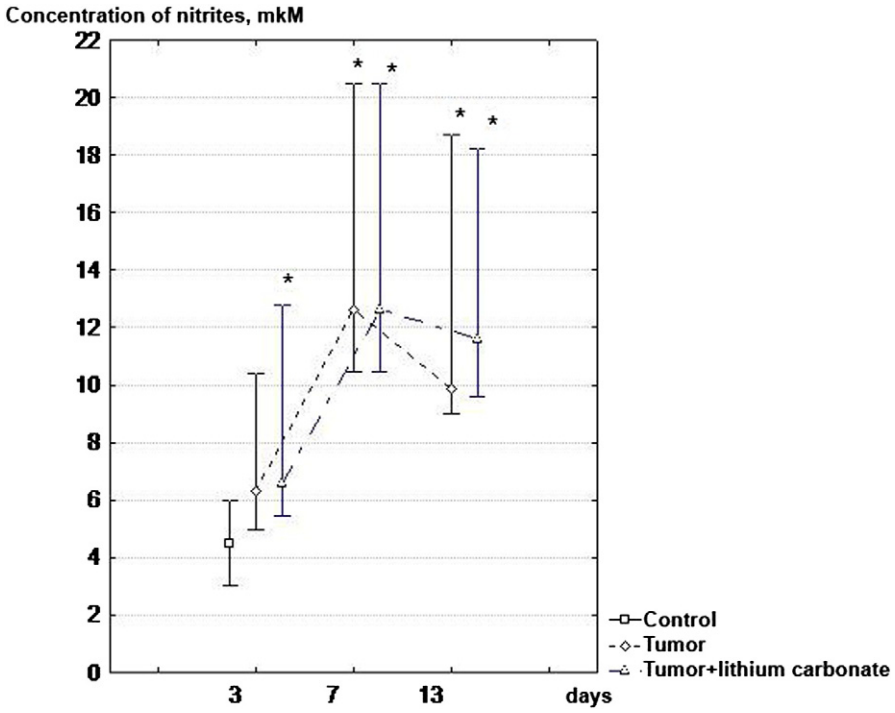


**Fig. 6.** Dynamics of NO production by peritoneal macrophages, with hepatocellular carcinoma (H-29) development in muscular tissue of right thigh under conditions of correction using lithium carbonate nano-scaled particles. * — $P < 0.05$ compared with the group of intact animals.

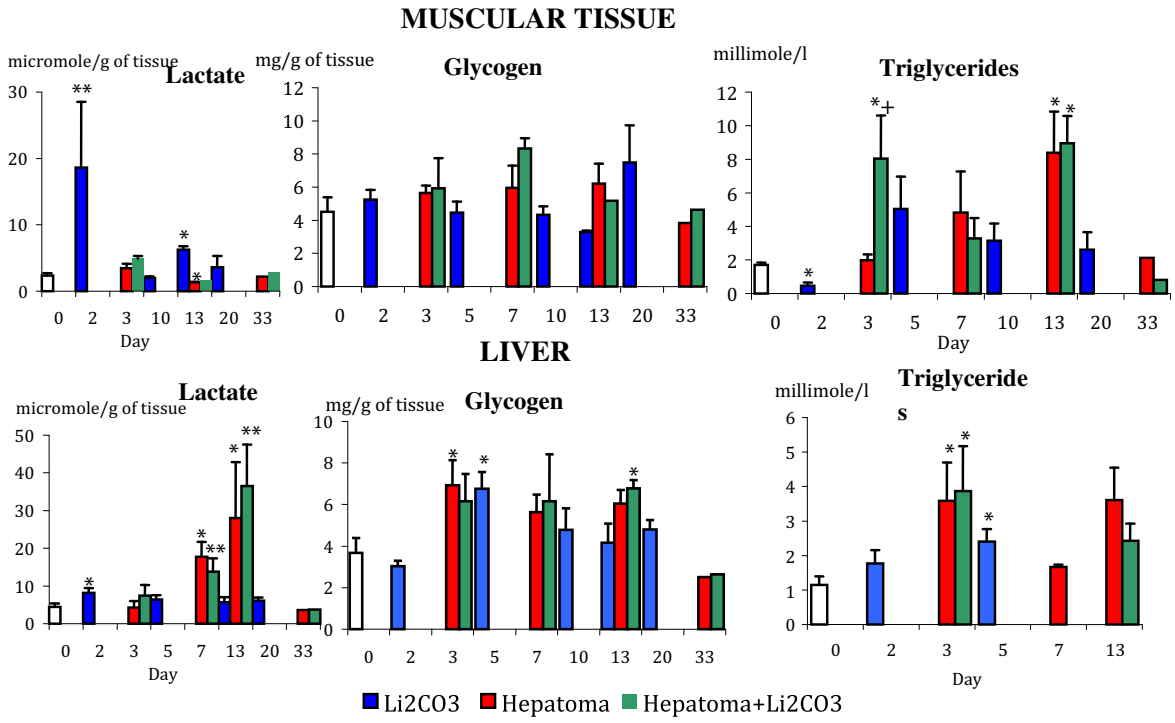


**Fig. 7.** Metabolic changes in muscular tissue and liver under conditions of tumour growth and impact of lithium carbonate nano-scaled particles. * — $P < 0.05$ compared with control.

proliferation was accompanied by an increase in intracellular lipids (triglycerides, total cholesterol, free cholesterol) and fatty acid concentration (Igarashi and Miyazawa, 2001). These results taken together show that changes in metabolism of fatty acids influenced on intensity of tumour cells' proliferation.

Lactic acid concentrations in the liver increased gradually in animals with spontaneous development of tumour process in muscular tissue caused by the inoculation of hepatocellular carcinoma cells. On the 7th day of hepatocellular carcinoma development, the concentration of lactate in the liver exceeded control values 3.9 times, and on the 13th day, it exceeded control values 6.2 times (Fig. 7). This argued for activation of anaerobic glycolysis process and for development of anaemia hypoxic syndrome. Under conditions lacking oxygen, mitochondrial breathing in cells reduces and ATP is produced by anaerobic glycolysis. Hypoxia-inducible factor, a regulator of transcription for glucose metabolism enzymes (Pescador et al., 2010), plays the key role in this metabolic shift. In the liver, lactate usually turns into glucose, and then through glycogenesis turns into glycogen. During our experiment, the level of glycogen almost doubled — becoming 1.9 times higher compared with the reference level from day three of hepatocellular carcinoma development (Fig. 7). The study showed that hypoxia can lead to accumulation of glycogen by enhancement of glucose flux in the cell. This occurs due to an increase in the level of a transporter protein, GLUT-1 and glucose's participation in its biosynthesis by activation of glycogen synthase (Pescador et al., 2010). This mechanism is confirmed by cell culture studies, which were performed on myocytes, normal hepatocytes and cells of different hepatomas. Glycogen accumulation in cells improves their survivability under hypoxia. During subsequent time-points in our study, the level of glycogen in liver tissue did not significantly differ from the control group.

This study has shown that excess glucose enters into systemic circulation and was consumed more not by the tumour tissue, but by other tissues because their metabolism switched to glucose's consumption due to lack of oxygen provision. In addition, excess glucose was likely converted into triglycerides by the liver, as seen by the day three concentration of triglycerides being 3.1 times higher than its rate in group of intact animals. Triglyceride accumulation in muscular tissue in the area inoculated by tumour cells can also be explained by significant decreases in lipase, which decomposes neutral fats. Patients with liver cancer development experience damage of liver cells, and activity of lipase, which hydrolyses triglycerides, goes down (Hiraoka et al., 1993). Correction of hepatocellular carcinoma-29, developing in muscular tissue, by lithium carbonate nano-scaled particles did not influence the intensity of anaerobic glycolysis or accumulation of glycogen and triglycerides in the liver because the dynamics of lactate, glycogen and triglycerides concentration was the same as for animals with spontaneous tumour development (Fig. 7).

## Conclusion

During the first two weeks of tumour process development in which lithium carbonate nano-scaled particles were introduced, we monitored the activation of the drainage-detoxification function of regional to tumour lymph node and metabolic processes in muscular tissue and liver. Under conditions of tumour process progression, the protective barrier functions of the lymph nodes gradually decreased. By the 30th day of the experiment, tumour cells disseminated into regional lymph nodes and the liver. Single and multiple doses of lithium carbonate nano-scaled particles on the periphery of tumour growth did not result in the removal of tumour cells from the thigh muscular tissue. We also noted in the early stages after introduction that there was an increase of macrophages and neutrophils within the tumour, a decrease in blood microvessel density and haemoglobin and an increase of tumour cell necrosis rate. Then, in the late stages of tumour development there were destructive changes occurring in the cytoplasm and nuclei of tumour cells. During tumour process development, neither single nor five-fold introduction of lithium nano-scaled particles affected NO production by peritoneal macrophages. Correction of tumour process by lithium carbonate nano-scaled particles inhibited activity of lipid peroxidation processes in tissue which was affected by hepatocellular carcinoma by inoculation. However, it did not impact the activity of antioxidant enzymes such as catalase and superoxide dismutase. The introduction of lithium carbonate nano-scaled particles into the area of tumour growth protected vital organs such as the heart and lungs from the damaging effect of lipid peroxidation afterproducts.

## References

Bgatova, N.P., Makarova, O.P., Pozhidayeva, A.A., Borodin, Y.I., Rachkovskaya, L.N., Konenkov, V.I., 2012. Biological effects of lithium nano-scaled particles. Achiev. Life Sci. 5, 29–46.

Canales, M.A., Arrieta, R., Hernandez-Garcia, C., Bustos, J.G., Aguado, M.J., Hernandez-Navarro, F., 1999. A single apheresis to achieve a high number of peripheral blood CD34+ cells in a lithium-treated patient with acute myeloid leukaemia. Bone Marrow Transplant. 23 (3), 305-305.

Corraliza, I.M., Campo, M.L., Soler, G., Modolell, M., 1994. Determination of arginase activity in macrophages: a micromethod. J. Immunol. Methods 174, 231–235.

Golokhvastov, K.S., Bgatova, N.P., Seagull, V.V., Panichev, A.M., Gulkov, F.N., 2013. Effect of nano and microparticles zeolites on immune response for different routes of administration. Russ. Immunol. J. 7 (2–3), 183–184.

Hager, E.D., Dziambor, H., Hohmann, D., Winkler, P., Strama, H., 2001. Effects of lithium on thrombopoiesis in patients with low platelet cell counts following chemotherapy or radiotherapy. Biol. Trace Elem. Res. 83 (2), 139–148.

Hager, E.D., Dziambor, H., Winkler, P., Hohmann, D., Macholdt, K., 2002. Effects of lithium carbonate on hematopoietic cells in patients with persistent neutropenia following chemotherapy or radiotherapy. J. Trace Elem. Med. Biol. 16 (2), 91–97.

Hiraoka, H., Yamashita, S., Matsuzawa, Y., Kubo, M., Nozaki, S., Sakai, N., Hirano, K., Kawata, S., Tarui, S., 1993. Decrease of hepatic triglyceride lipase levels and increase of cholesteryl ester transfer protein levels in patients with primary biliary cirrhosis: relationship to abnormalities in high-density lipoprotein. Hepatology 18 (1), 103–110.

Igarashi, M., Miyazawa, T., 2001. The growth inhibitory effect of conjugated linoleic acid on a human hepatoma cell line, HepG2, is induced by a change in fatty acid metabolism, but not the facilitation of lipid peroxidation in the cells. Biochim. Biophys. Acta 1530 (2–3), 162–171.

Kaledin, V.I., Zhukova, N.A., Nikolin, V.P., Popova, I.A., Belyaev, M.D., Baginskaya, N.V., Litvinova, E.A., Tolstikova, T.G., Lushnikova, E.L., Semenov, D.E., 2009. Hepatocellular carcinoma-29 — metastazing transplantable mice's tumor calling cachexia. Bull. Exp. Biol. Med. 148 (12), 664–669.

Khasraw, M., Ashley, D., Wheeler, G., Berk, M., 2012. Using lithium as a neuroprotective agent in patients with cancer. BMC Med. 10 (131), 1–7.

Kudo, M., 2012. Treatment of advanced hepatocellular carcinoma with emphasis on hepatic arterial infusion chemotherapy and molecular targeted therapy. Liver Cancer 1 (2), 62–70.

Lee, J.E., Bae, S.H., Choi, J.Y., Yoon, S.K., You, Y.K., Lee, M.A., 2014. Epirubicin, Cisplatin, 5-FU combination chemotherapy in sorafenib-refractory metastatic hepatocellular carcinoma. World J. Gastroenterol. 20 (1), 235–241.
Lowry, O.H., Rosebrough, N.J., Farl, A.L., Randall, R.J., 1951. Protein measurement with the Folin phenol reagent. J. Biol. Chem. 193 (1), 265–275.
Menshchikova, E.B., Zenkov, N.K., Lankin, V.Z., Bondar, I.A., Trufakin, V.A., 2008. Oxidative Stress: Morbid Condition and Diseases. Artra, Novosibirsk.
Merendino, R.A., Mancuso, G., Tomasello, F., Gazzara, D., Cusumano, V., Chillemi, S., Spadaro, P., Mesiti, M., 1994. Effects of lithium carbonate on cytokine production in patients affected by breast cancer. J. Biol. Regul. Homeost. Agents 8 (3), 88–91.
Mo, M., Erdelyi, I., Szigeti-Buck, K., Benbow, J.H., Ehrlich, B.E., 2012. Prevention of paclitaxel-induced peripheral neuropathy by lithium pretreatment. FASEB J. 26 (11), 4696–4709.
Nepomnyashchikh, L.M., Lushnikova, E.L., Molodykh, O.P., Klinnikova, M.G., 2005. Ultrastructural manifestations of cardiac hystiocytes regeneration disturbance under effect of doxorubicin. Morphology 4, 81–84.
Nepomnyashchikh, L.M., Lushnikova, E.L., Molodykh, O.P., Klinnikova, M.G., 2006. Structural reorganization of rats' livers under cytotoxic action of doxorubicin. Bull. Exp. Biol. Med. 141 (5), 579–585.
Pang, R.W., Poon, R.T., 2012. Cancer stem cell as a potential therapeutic target in hepatocellular carcinoma. Curr. Cancer Drug Targets 1 (2(9)), 1081–1094.
Pescador, N., Villar, D., Cifuentes, D., Garcia-Rocha, M., Ortiz-Barahona, A., Vazquez, S., Ordonez, A., Cuevas, Y., Saez-Morales, D., Garcia-Bermejo, M.L., Landazuri, M.O., Guinovart, J., Del, P.L., 2010. Hypoxia promotes glycogen accumulation through hypoxia inducible factor (HIF)-mediated induction of glycogen synthase 1. PLoS ONE 5 (3), 1–13.
Shen, Y., Cao, D., 2012. Hepatocellular carcinoma stem cells: origins and roles in hepatocarcinogenesis and disease progression. Front. Biosci. (Elite Ed.) 1 (4), 1157–1169.
Tiuryaeva, I.I., Filatova, N.A., Rozanov, I.M., Demin, C.I., Blinova, G.I., Ivanov, V.A., 2010. Morphological and functional heterogeneity of rat's ascite Zajdel hepatoma cells. Tsitologiya 52 (10), 817–826.
Tono, T., Hashimoto, K., Yamada, Y., Nishida, K., Yanagawa, T., Danno, K., Fujie, Y., Fujita, S., Fujita, J., Yoshida, T., Onishi, T., Imaoka, S., Monden, T., 2013. Efficacy of stereotactic radiotherapy for primary and metastatic liver cancer. Gan To Kagaku Ryoho 40 (12), 1853–1855.
Volchegorsky, I.A., Dolgushin, I.I., Kolesnikov, O.L., Ceylikman, V.E., 2000. Experimental Modeling and Laboratory Estimation of Organism's Adaptive Mechanisms. Chelyabinsk State Pedagogical University Press, Chelyabinsk.
Wang, J.S., Wang, C.L., Wen, J.F., Wang, Y.J., Hu, Y.B., Ren, H.Z., 2008. Lithium inhibits proliferation of human esophageal cancer cell line Eca-109 by inducing a $G_2$/M cell cycle arrest. World J. Gastroenterol. 14 (25), 3982–3989.
Wolff, E.F., Hughes, M., Merino, M.J., Reynolds, J.C., Davis, J.L., Cochran, C.S., Celi, F.S., 2010. Expression of benign and malignant thyroid tissue in ovarian teratomas and the importance of multimodal management as illustrated by a BRAF-positive follicular variant of papillary thyroid cancer. Thyroid 20 (9), 981–987.
Yang, E.S., Lu, B., Hallahan, D.E., 2007. Lithium-mediated neuroprotection during cranial irradiation: a phase I trial. I. J. Radiat. Oncol. 69 (1), 586–587.
Zhang, L., Zhu, H., Jin, C., Zhou, K., Li, L., Su, H., Chen, W., Bai, J., Wang, Z., 2009. High-intensity focused ultrasound (HIFU): effective and safe therapy for hepatocellular carcinoma adjacent to major hepatic veins. Eur. Radiol. 19 (2), 437–445.
Zhu, Q., Yang, J., Han, S., Liu, J., Holzbeierlein, J., Thrasher, J.B., Li, B., 2011. Suppression of glycogen synthase kinase 3 activity reduces tumor growth of prostate cancer in vivo. Prostate 71 (8), 835–845.